Available online at www.sciencedirect.com
SCIENCE DIRECT®
Biochemical and Biophysical Research Communications 327 (2005) 163–173
BBRC
www.elsevier.com/locate/ybbrc

Selenium-induced alterations in ionic currents of rat cardiomyocytes

Murat Ayaz[a], Semir Ozdemir[a], Nazmi Yaras[a], Guy Vassort[b], Belma Turan[a,*]

[a] Departments of Biophysics, School of Medicine, Ankara University, 06100 Ankara, Turkey
[b] INSERM U-637, Physiopathologie Cardiovasculaire, CHU Arnaud de Villeneuve, Montpellier, France

Received 25 November 2004
Available online 9 December 2004

Abstract

In the present study, rats were treated with sodium selenite (5 μmol/kg body weight/day, ip) for 4 weeks and the parameters of contractile activity, action potential, L-type Ca^{2+}-current (I_{CaL}), as well as transient outward (I_{to}), inward rectifier (I_{K1}), and steady state (I_{ss}) K^+-currents were investigated. Sodium selenite treatment increased rat blood glucose level and lowered plasma insulin level, significantly. This treatment also caused slightly prolongation in action potential with no significant effects on spontaneous contraction parameters and intracellular Ca^{2+} transients of the heart preparations. These effects were associated with marked alterations in the kinetics of both I_{CaL} and I_{to} including a significant slowing in both inactivation time constants of I_{CaL} and a significant shift to negative potential at half-inactivation of these channels without any change in the current density. Also, there was a significantly faster inactivation of I_{to} and no shift in half-inactivation of this channel without any change in its current density. Consequently, there was a ~50% increase in total charges carried by Ca^{2+} current and ~50% decrease in total charges carried by K^+ currents of the treated rat cardiomyocytes. Additionally we observed a significant inhibition in I_{K1} density in treated rat cardiomyocytes. Oxidized glutathione level was significantly increased (70%) while the observed decrease in reduced glutathione was much less. Since a shift in redox state of regulatory proteins is related with cell dysfunction, selenium-induced increase in blood glucose and decrease in plasma insulin may correlate these alterations. These alterations, in the kinetics of the channels and in I_{K1} density, might lead to proarrhythmic effect of chronic selenium supplementation.

Keywords: Sodium selenite; Calcium current; Potassium current; Contraction; Action potential; Intracellular free Ca^{2+} concentration

The trace element selenium (Se), a component of glutathione peroxidase (GSHPx), is known today to be an essential element in the mammalian diet, and sodium selenite is commonly used as a dietary supplement for the treatment of selenium deficiency [1,2]. Parallel to the discovery of the molecular biology of selenoproteins, it became apparent that Se levels differentially control selenoprotein expression in certain tissues [3]. This tissue-specific hierarchy for Se intake levels indicates that specific Se uptake or retention mechanisms exist even under suboptimal nutritional conditions.

There are several epidemiological studies linking low serum selenium levels to coronary artery disease [4–6]. Selenium supplementation has been suggested to the people who have deficiency states; indeed, a protective effect of selenium during myocardial ischemia has been reported [7]. So, the role of Se as an antioxidant agent prompted the investigators to study the effect of Se on the functions of several organs under pathological conditions with the aim of developing new Se-based pharmaceutical agents [8,9]. It is known that Se compounds can restore some metabolic parameters in experimental diabetes, and recently we have shown beneficial effects of sodium selenite in altered diabetic cardiac functions [10]. When streptozotocin-induced diabetic rats were

* Corresponding author. Fax: +90 312 3106370.
E-mail address: bturan@medicine.ankara.edu.tr (B. Turan).

0006-291X/$ - see front matter © 2004 Elsevier Inc. All rights reserved.
doi:10.1016/j.bbrc.2004.12.003

treated with sodium selenite (5 μmol/kg body weight/day) for 4 weeks, prolongation in both action potential duration and twitch duration of papillary muscle as well as diminished amplitudes of the K^+ currents could be reversed significantly.

Although Se compounds are known to play an antioxidant role in mammalians, their effects are likely to be concentration and tissue dependent, and the effects of sodium selenite on heart function have yet to be characterized in detail. Experimental chronic Se toxicity in animals affects the major organs; more particularly, sodium selenite has been shown to cause cellular dysfunction in tissues [11–13].

Our very recent in vitro data indicated that addition of sodium selenite (75–100 nM) into perfusion solution has protective role against ischemia–reperfusion-induced myocardial injury due to its effect on both the ratio of reduced glutathione to oxidized glutathione (GSSG) and ratio of phospho-NFκB of particulate to homogenate of the heart preparations [14]. It is almost clear that while low concentrations of Se are essential for the synthesis of selenocysteine-containing enzymes [15], an excess of Se is also toxic to both animals and human, and many Se compounds are potent prooxidant, and/or oxidants. So, the effects of Se on muscle function are controversial yet.

Considering the importance of sodium selenite as a supplement in deficiency and its possible specific effects in protein thiols, the present study aimed at characterizing its action on normal rat heart function in detail. So, we investigated the effect of sodium selenite treatment of normal rats for 4 weeks on Ca^{2+}- and K^+-currents, action potential parameters, intracellular free Ca^{2+} concentration ($[Ca^{2+}]_i$), and contraction parameters as well as the levels of glutathione, lipid peroxidation, nitric oxide, and levels of other enzymes which play important role in antioxidant defense system of the cell.

Materials and methods

Animal groups

In this study, we used two groups: control (untreated) group and sodium selenite-treated group. Wistar rats of both sexes weighing 200–250 g (12–14 weeks) were used for the experiments. Animals were separated depending on their sex and housed three rats per cage, and fed with standard rat nutrient and water without restriction throughout the experiment. Treated group of rats received sodium selenite (5 μmol/kg body weight/day) intraperitoneal (ip) injection while control group received comparable volume of daily saline injections (ip) for 4 weeks.

Body weights and blood glucose levels were measured before and at different times after the injection. Blood glucose level of all animals was measured using a glucose analyzer (Glucotrend, Roche). Plasma selenium level was measured with graphite-furnace atomic absorption spectrometer (AA-30/40 Varian atomic absorption spectrometer).

Measurement of action potential

Rats were anesthetized with pentobarbital sodium (30 mg/kg body weight, ip) and the hearts were excised rapidly. Papillary muscles of the left ventricle were excised under binocular microscope, placed in a chamber, and pinned down at one end with a stimulating electrode while the second end was connected to a force-displacement transducer (FT-03, Grass Instruments). The dimensions of the papillary muscle strips were similar in between the groups. The recording chamber was perfusated with Krebs solution gassed with 95% O_2–5% CO_2 and maintained at 37 °C. Composition of the Krebs solution was (mM): 119 NaCl, 4.8 KCl, 1.8 $CaCl_2$, 1.2 $MgSO_4$, 1.2 KH_2PO_4, 20 $NaHCO_3$, and 10 glucose (pH 7.4). Intracellular action potentials were measured using a conventional glass microelectrode filled with 3-M KCl (15–20 MΩ) connected to a preamplifier (P16, Grass Instruments). The muscle strips were stimulated by using rectangular electrical pulses 3 ms in duration at a frequency of 0.2 Hz (S48, Grass Instruments). Action potential data were transferred to a PC through an A/D converter and evaluated by a homemade program. Parameters for the action potential repolarization phase ($APD_{25,\ 50,\ 90}$) were calculated from AP traces and compared between groups.

Langendorff-perfused heart preparation

After rats had been anesthetized with sodium pentobarbital (30 mg/kg body weight, ip), hearts were rapidly removed and placed in cold, low-Ca^{2+}-containing modified Krebs solution (in mM): 120 NaCl, 5.0 KCl, 0.63 $CaCl_2$, 1.2 $MgCl_2$, 2.0 NaH_2PO_4, 1.2 Na_2SO_4, 20 $NaHCO_3$, 10 glucose, and 20 Hepes, pH 7.4, and gassed with 95% O_2 and 5% CO_2. In other experiments the Langendorff-perfused heart was prepared for recording isometric force by attaching one end to a fixed arm and the other to a force-displacement transducer (Grass Model FT-03) and perfused with Krebs solution containing 1.3-mM $CaCl_2$. Spontaneous contractions and their time derivatives were recorded on a two-channel polygraph (Grass model 79D). All preparations were allowed to equilibrate for 40–50 min. All experiments were performed at 37 °C.

Ventricular cell isolation

Rats were anesthetized with heparinized pentobarbital sodium (30 mg/kg body weight, ip) and the hearts were removed rapidly. The aorta was cannulated on a Langendorff apparatus and perfused retrogradely through the coronary arteries at 37 °C. A Ca^{2+}-free solution was passed through (3–5 min) to clean out the remaining blood. The composition of the solution was as follows (mM): 145 NaCl, 5.0 KCl, 1.2 $MgSO_4$, 1.4 Na_2HPO_4, 0.4 NaH_2PO_4, 5.0 Hepes, and 10 glucose (bubbled with 100% O_2, pH 7.4). This was followed by perfusion with this solution added with 1 mg/ml collagenase (Collagenase A, Boehringer–Mannheim) for ~35 min. The ventricles were then removed and minced into small pieces prior to filtration. The percent of viable cells was more than 70% in all groups. Subsequently, Ca^{2+} level in the medium was increased in a graded manner to a concentration of 1.3 mM.

Voltage-clamp recording: pulse protocol and data analysis

Potassium currents. The bathing solution for K^+ currents contained (in mM): 136, NaCl, 5.5 KCl, 1.0 $MgCl_2$, 10 Hepes, 0.5 $CaCl_2$, 11 glucose, pH adjusted to 7.4 with NaOH, and pipette solution contained (in mM): 80 L-aspartic acid, 10 KH_2PO_4, 1.0 $MgSO_4$, 50 KCl, 5.0 Hepes, 5.0 ATP-Na_2, and 10 EGTA-K, pH adjusted to 7.4 with KOH.

Recording of the K^+ currents was performed at room temperature (22 ± 2 °C) using the whole-cell configuration of the patch-clamp technique as described earlier [10,16]. The electrode resistance was 1.0–

1.2 MΩ. K^+ currents were recorded (see below 0.14 Hz) using a patch-clamp amplifier (Model RF-300; Biologic, Claix, France) and filtered at 3 kHz. Current traces were digitized at 5 kHz using Digidata 1200 and analyzed using pClamp 8 software (Axon Instruments, Foster City, CA, USA).

K^+ currents were recorded in the presence of external Cd^{2+} (250 μM) to inhibit Ca^{2+} current. To inactivate the sodium current, cells were first depolarized to −50 mV and held at −50 mV for 50 ms before each test depolarization was applied. From a holding potential (HP) of −80 mV, voltage pulses (duration of 600 ms) between −120 and +70 mV (with 10 mV steps) were applied at a frequency of 0.14 Hz. K^+ currents were normalized with cell capacitance and expressed as pA/pF. A detailed kinetic analysis of the I_{to} was performed. I_{to} activation characteristic was determined by applying 6 ms prepulses within the range −40 to +50 mV in 10 mV increments that were followed by a −40 mV, 120 ms pulse. Its inactivation was established by applying a 200 ms prepulse within the range −85 mV to +30 mV in 10 mV increments that was followed by a +50 mV pulse 300 ms long. During another protocol, two pulses (+50 mV, 500 ms) with increasing interval durations (20–300 ms) were used to determine the reactivation curve. Boltzmann functions were used to fit activation ($I/I_{max} = [1 + \exp(V_{1/2} - V_m)/k]^{-1}$) and inactivation ($I/I_{max} = [1 + \exp(V_m - V_{1/2})/k]^{-1}$) curves.

L-type calcium current. Ca^{2+} currents were recorded at room temperature (22 ± 2 °C) using the whole-cell configuration of the patch clamp technique. Sodium currents were inactivated by voltage ramp to −50 mV from a holding potential of −80 mV [12,16]. The electrode resistance was 1.0–1.2 MΩ.

Pipette solution for Ca^{2+} currents contained (in mM): 110 Cs-aspartate, 20 CsCl, 1.0 $MgCl_2$, 5.0 phosphocreatine-Na_2, 5.0 ATP-Na_2, 10 EGTA-K, and 5.0 Hepes (pH 7.4). The bathing solution for Ca^{2+} currents contained (in mM): 120 NaCl, 1.7 $MgCl_2$, 20 $CsCl_2$, 10 Hepes, 1.8 $CaCl_2$, 11 glucose, pH adjusted to 7.4 with NaOH. Ca^{2+} currents were recorded from a HP of −80 mV, after a ramp to −45 mV, using 250-ms depolarizing pulses to potentials between −50 and +60 mV (with 10 mV step increment) applied at a frequency of 0.2 Hz. Current amplitude was estimated as the difference between peak inward current and the current level at the end of the pulse. Current/voltage relationships and availability curves were constructed using a standard pulse voltage protocol. Current amplitudes elicited by the test pulse normalized to the maximal current were plotted as a function of prepulse potentials to give the availability curve. The inactivation time course of currents was calculated by fitting the curve traces by a two exponential equation ($y = A*\exp(-t/\tau_f) + B*\exp(-t/\tau_s)$).

Mathematical model of action potential

In this part of the study the activation and inactivation parameters of all ionic currents, except those measured by us, were taken from a recently published mathematical model [17–19].

Density of Na^+ current kept unchanged in mathematical models applied to groups. The kinetics of I_{to} and the density of I_{K1} are altered in sodium selenite treated rat cardiomyocytes according to our experimental records. I_{CaL} density was not changed but its kinetics was significantly altered following our experimental data. Parameters of other currents used in the model were taken from the mathematical model of Pandit et al. [17]. Model conditions, extracellular ionic concentrations and temperature (22 ± 2 °C), were assumed to be equal with experimental conditions and set to same values for all model groups. The membrane capacitance was assigned to 100 pF in this model study.

Intracellular free Ca^{2+} measurements

The intracellular Ca^{2+} level was measured by fura-2 fluorescence. Cells were kept in the control medium for 3 h before the experimental procedure. They were then incubated for 50 min with 4 μM fura-2 AM for loading. Fluorescence was recorded using a PTI Ratiomaster spectrophotometer coupled to the microscope using 340/380 nm excitation and 510 nm emission wavelengths. The ratio of the emitted fluorescence at 340 and 380 nm excitations was used as indicator of the free $[Ca^{2+}]_i$. $F_{340/380}$ was sampled at a frequency of 20 Hz.

The composition of the bath solution was as follows (mM): 130 NaCl, 4.8 KCl, 1.2 $MgSO_4$, 1.5 $CaCl_2$, 1.2 KH_2PO_4, 10 Hepes, and 10 glucose (pH 7.4). Following recording of resting $[Ca^{2+}]_i$ fluorescence for 20 s, field stimulation with 30-V, 10-ms pulses at 0.2 Hz were applied. Resting ratio, amplitude (difference between basal and peak $F_{340/380}$ ratios), time to peak (TP), and time to half-decay (DT_{50}) of the Ca^{2+} transients were determined. Background fluorescence measured on a cell-free field was subtracted from all recordings prior to the calculation of ratios.

Biochemical assays

Sample preparation. Tissues for antioxidant enzyme section were homogenized and centrifuged at 18,000*g* for 60 s at 4 °C. The resulting supernatants were collected and stored at −85 °C until analysis. The weighted other part of heart tissues was homogenized in 0.25 M sucrose solution, centrifuged at 18,000*g* for 20 min at 4 °C, and the supernatant was stored in ultracold. Total protein assay of homogenates was performed according to Lowry [20]. All the enzyme activities of each sample were normalized per milligram of protein.

Lipid peroxidation (LPO). Assay was based on the reaction of a chromogenic reagent, *N*-methyl-2-phenylindole, with MDA and 4-hydroxyalkenals at 45 °C. One molecule of either MDA or 4-hydroxyalkenal reacts with 2 molecules of reagent *N*-methyl-2-phenylindole in acetonitrile to yield a stable chromophore with maximum absorbance at 586 nm.

Superoxide dismutase. The measurement was based on the superoxide dismutase (SOD)-mediated increase in the rate of autoxidation of 5,6,6a,11b-tetrahydro-3,9,10-rihydroxybenzo[c]fluorene (diethylenetriaminepentaacetic acid) in aqueous alkaline solution to yield a chromophore with maximum absorbance at 525 nm. The SOD activity was determined from the ratio of the autoxidation rates in the presence and absence of SOD. The ratio as a function of SOD activity is independent of the type SOD (Cu/Zn-SOD, Mn-SOD, and Fe-SOD) being measured [21].

Glutathione reductase. The measurement was based on the oxidation of NADPH to $NADP^+$ which was catalyzed by a limiting concentration of glutathione reductase (GR). One molecule of NADPH is consumed for each molecule of GSSG to reduce. Therefore, the reduction of GSSG is determined indirectly by the measurement of the consumption of NADPH, as demonstrated by a decrease in the absorbance at 340 nm as a function of time.

Glutathione peroxidase. Assay was an indirect measure of the activity of c-GSHPx [22]. GSSG produced upon reduction of organic peroxide by c-GSHPx is recycled to its reduced state by the enzyme GR. To assay c-GSHPx, tissue homogenates were added to the solution containing glutathione, GR, and NADPH. Enzyme reaction was initiated by adding the substrate of *tert*-butyl hydroperoxide. The absorbance was recorded at 340. The rate of decrease in the absorbance is directly proportional to the GSHPx activity in the sample.

Total glutathione (G). The measurement method was based on the formation of a chromophoric thione (French Patent No. 9115868, United States Patent 5,817,520). The absorbance measured at 420 nm is directly proportional to the GSH concentration. There are three steps to the reaction. First, the sample is buffered and the reducing agent, tris(2-carboxyethyl)phosphine (TCEP) [23], is added to reduce any oxidized glutathione (GSSG) to the reduced state. The chromogen, 4-chloro-1-methyl-7-trifluoromethylquinolinium methylsulfate, is added forming thioethers with all thiols present in the sample. Upon addition of base which raises the pH to greater than 13, a β-elimination specific to the GSH-thioether results in the chromophoric thione.

Reduced glutathione. Reduced glutathione (GSH) concentrations were determined by the procedure of Ellman [24]. Briefly, 0.5 ml

homogenate, 1.5 ml of 0.15 M KCl, and 3 ml deproteinization solution were mixed. Each sample was centrifuged at 3.000 rpm for 10 min and supernatant was removed following which 2 ml phosphate solution and 0.5 ml DTNB were added to the 0.5 ml supernatant. Absorbance was read at 412 nm and compared with glutathione standards. The amount of GSSG was calculated by subtracting measured GSH from measured G.

Nitric oxide products (NOPs). The measurement was based on the determination of nitrite. Spectrophotometrical determination of nitrite using Greiss reagent is straightforward and sensitive, but does not measure nitrate, causing a possible underestimation of nitric oxide. In order to eliminate the underestimation, granular cadmium metal for chemical reduction of nitrate to nitrite was done. In acid solution, nitrite is converted to nitrous acid (HNO_2) which diazotizes sulfanilamide. This sulfanilamide-diazonium salt is then reacted with *N*-(1-naphthyl)-ethylenediamine (NED) to produce a chromophore which is measured at 540 nm.

Chemicals and statistical evaluation of data

All chemicals used were purchased from Sigma (Sigma–Aldrich Chemie, Steinheim, Germany) except collagenase A, which was from Boehringer–Mannheim (Roche Diagnostics, Mannheim, Germany). All the biochemical measurements were carried out by OxisResearch test kits.

Groups were compared using Student's *t* test. p values <0.05 were taken as significant, and significance levels were given in the text. Data are presented as average ± SEM, throughout the text.

Results

General effects

At the end of the 4-week experimental period, sodium selenite treatment did not affect the weight gain and heart size of the animals nor did it affect the cell size estimated from cell capacitance (Table 1). Blood glucose levels were increased slightly but significantly ($p < 0.05$) in sodium selenite-treated rats with respect to the untreated controls.

After four weeks of sodium selenite treatment of the rats, the plasma selenium level had increased by about 10% with respect to the control value although this was not significant. Surprisingly it is to note that in a previous study [10], sodium selenite treatment caused a more than 2-fold decrease in plasma insulin level from 109.2 ± 15.2 to 281.6 ± 57.3 fmol/ml.

Effects of sodium selenite treatment on action potential parameters

Typical action potential recordings in a control and a selenium-treated rat heart papillary muscle using microelectrode are illustrated in Fig. 1A (inset). The mean resting membrane potentials of untreated and treated cells were -83.0 ± 0.6 and -80.6 ± 1.1 mV, respectively, while the maximum depolarization potentials of these two groups were 12.9 ± 0.7 and 13.9 ± 1.2 mV, respectively. On average, there was no significant difference between resting membrane potential and peak voltage (maximum depolarization potential) values of the two groups of animals. Durations of the action potential repolarization phase ($APD_{25,\ 50,\ 90}$) were calculated and compared between these two groups (Fig. 1A). Despite, the mean value of APD_{90} in the treated group (81.7 ± 5.8 ms) being higher than in the untreated group (71.0 ± 3.6 ms), the difference between these two groups was not statistically significant ($p > 0.05$).

Effects of sodium selenite treatment on contractile activity of papillary muscle

We measured the maximum force of spontaneous contraction, heart rate, rate of tension development ($+dT/dt$), and rate of relaxation ($-dT/dt$) in Langendorff-perfused hearts, for baseline contractions. The mean values of maximum force of contraction were not significantly different between sodium selenite-treated and -untreated groups (Fig. 1B). Also the mean values for rate of tension development ($+dT/dt$) and rate of relaxation ($-dT/dt$) appear not to be statistically significant between these two groups (Fig. 1C). Shortly, sodium selenite treatment of the rats did not significantly alter any parameters of the spontaneously beating heart.

Sodium selenite treatment alters kinetics of L-type calcium current

Typical L-type Ca^{2+} currents, I_{CaL} recordings in a control and a selenium-treated rat heart myocytes using whole-cell configuration of patch-clamp technique are

Table 1
Characteristics of the rats with or without sodium selenite treatment

	Body weight (g)		Blood glucose (mg/dL)		Cell capacitance (pF)	Plasma selenium (ng/ml)
	Initial	Final	Initial	Final		
Control	222.3 ± 2.1	235.2 ± 1.8	101.0 ± 1.0	101.2 ± 0.6	142.5 ± 7.5	113.5 ± 16.5
	($N = 46$)		($N = 46$)		($N = 10$)	($N = 8$)
Se-treated	220.4 ± 1.6	234.9 ± 2.1	100.8 ± 0.5	129.2 ± 3.5*	142.8 ± 11.6	126.7 ± 5.8
	($N = 47$)		($N = 47$)		($N = 12$)	($N = 7$)

Values are means ± SEM. Control group, saline-injected rats for four weeks; Se-treated group, sodium selenite-injected rats for four weeks. *N* represents the number of animals. Start and end are representing the initial and final situations of the animals during experimental protocol.

* $p < 0.05$ is the significance levels compared to the control group.

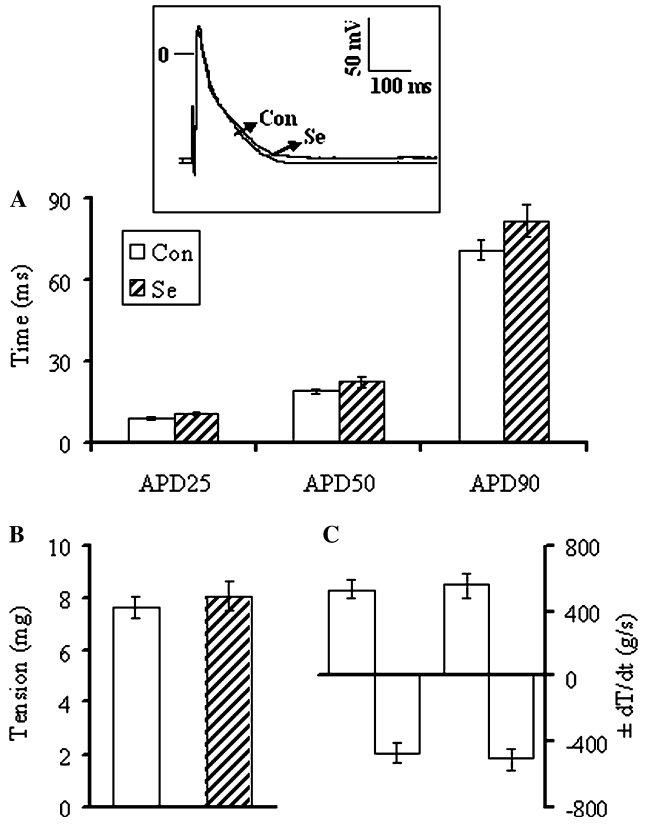

Fig. 1. Effect of sodium selenite treatment on action potential and spontaneous beating parameters of heart preparations. (A) Representative intracellular action potential recordings from papillary muscle strips (inset). Recordings from control (Con) and sodium selenite-treated control (Se) group animals. (B) Action potential duration 25, 50, 90 ($APD_{25,\ 50,\ 90}$) values measured from animals (10 rats with 33 impalements in control and 11 rats with 43 impalements in sodium selenite-treated control groups). (B) Maximum developed force of basal contraction, measured as grams. (C) Rate of tension development ($+dT/dt$) and relaxation ($-dT/dt$) as g/s (24 control and 15 selenite-treated rats). Values are represented as average ± SEM.

illustrated in Fig. 2A. I_{CaL} elicited at 0 mV from a holding membrane potential at −80 mV had similar amplitude (Fig. 2B) and exhibited slower inactivation time constants in both fast and slow parts (Fig. 2E). Particularly the difference in the late phase was more significant ($p < 0.001$) than in the fast phase ($p < 0.01$) although both of them were significantly different between these two groups of animals. This could indicate that some inward current was still flowing at the end of the 250 ms depolarization. Time-to-peak current was similar in both cell types (5.0 ± 0.4 and 5.0 ± 0.5 ms in control versus treated groups). Although slower inactivation time constants were generally associated with I_{CaL} of lesser amplitude, we have similar average amplitudes in these two groups. So, we calculated the quantity of total charges carried by the Ca^{2+} current over a 250 ms depolarizing period at 0 mV. As a result, the total carried charges at 0 mV in these two groups were 2.3 ± 0.1 amol/pF for the control group and 3.1 ± 0.3 amol/pF for the treated group (Fig. 2F). As shown in Fig. 2F, voltages between −20 and +30 carried charges were all significantly different from age matched control group animals.

As shown on the current–voltage relations of I_{CaL}, there were some shifts at −30 to −10 mV and +10 to +30 mV. Although there was no shift in the threshold voltages of both the control and the treated rat cells (Fig. 2B), the inactivation curves established on the two cell types were not completely superimposable (Fig. 2C). The potentials giving 50% of inactivation of these channels were -30.1 ± 0.5 mV for control cells and -33.2 ± 0.6 mV for the treated cells. There is about 10% difference (a shift to negative potentials) between these two groups and this difference was statistically significant ($p < 0.05$). Note however, the relief from inactivation of the channels following high-voltage prepulses was significantly larger in the treated rat cells. Percentage reactivation of the channels for both groups seemed similar to each other (Fig. 2D). There was no sign of a low threshold Ca^{2+} current in any of the cells investigated in the control or the treated rats.

Sodium selenite treatment induces alterations in potassium currents

To monitor K^+currents, cardiomyocytes were held at −80 mV in a cadmium containing solution to inhibit Ca^{2+}inward current. Three major K^+ currents, i.e., the transient outward current, I_{to}, the inward rectifier current, I_{K1}, and the steady-state outward current I_{ss}, were evaluated in the cardiomyocytes. Typical current traces from two groups are given in Fig. 3A. The current densities were estimated for I_{K1} at −120 mV, and for I_{to}, which was estimated as the difference between peak and steady currents elicited at +70 mV. Analysis of variance of the I_{to} density did not show significant difference between these two groups, despite I_{K1} density in the treated rat cells being significantly smaller than in the control rat cells (Fig. 3B). I_{to} recorded in the treated rat cardiomyocytes exhibited a shorter inactivation in slow part ($p < 0.05$) and no significant change in fast part (Fig. 3E). We could not have any significant effect on I_{ss} with sodium selenite treatment for 4 weeks (data not given).

Although shorter inactivation time constants were generally associated with I_{to} of higher amplitude, we recorded similar average amplitudes in these two groups. So, we calculated the quantity of total charges carried by the K^+ current over a 600 ms depolarizing period at +70 mV. As a result, the total carried charges at +70 mV in these two groups were 6.9 ± 0.6 amol/pF for the control and 5.0 ± 0.27 amol/pF for the treated group. Similarly, faster inactivation ends up with decreased charges carried by this current (Fig. 3F). Voltages between +10 and +70 mV, total carried charges

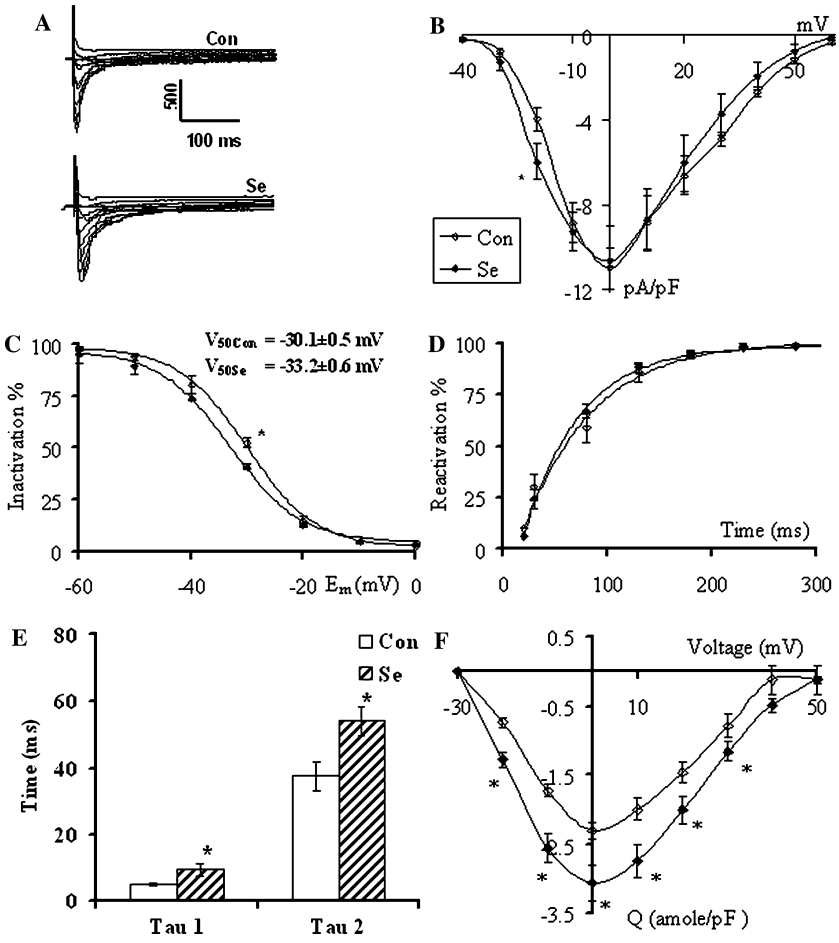

Fig. 2. Effect of sodium selenite treatment on I_{CaL} in ventricular cardiomyocytes. (A) Selected traces of I_{CaL} evoked by depolarization −50 mV from holding potential of −80 mV. (B) Current–voltage relationships of normalized I_{CaL} to membrane capacitance obtained from a holding potential of −80 mV (*N*, number of animals and *n*, number of cells are 5–17 and 5–18 in control and sodium selenite-treated control groups, respectively). (C) Graph is showing kinetics of the I_{CaL}. Steady-state inactivation curves obtained with two-pulse protocol. Holding potential was −80 mV. The currents resulting from the test pulse (0 mV, 250 ms) were normalized and plotted as a function of prepulse potential (duration 250 ms; range, −50 to +60 mV) from 17 normal cells (Con) and from 18 treated cells (Se). Note the rightward shift in I_{CaL} availability induced by selenium administration. (D) Time course of recovery from inactivation of I_{CaL} elicited with a two-pulse protocol is given. (E) shows charge–voltage relationships between the groups. All values are represented as average ± SEM, $*p < 0.05$ with respect to the control group.

by K^+ were significantly different from the control group.

As shown on the current–voltage relations (Fig. 3B), maximal peak current occurred at +70 mV in both the control and the treated rat cells, and the steady-state inactivation curves as well as the curves of recovery from inactivation of the K^+ channels established on the two cell types were superimposable (Figs. 3C and D).

Sodium selenite has no effect on intracellular free Ca^{+2}

To assess the effect of sodium selenite treatment on both intracellular Ca^{2+} transients and basal Ca^{2+} fluorescence intensity ratios (Fig. 4) in cardiomyocytes, we measured transients obtained by field stimulation in isolated cardiac cells, by using fluorescent indicator fura-2 (a representative trace in Fig. 4 inset). Transients measured in cardiomyocytes from the treated rat heart showed no considerable changes in the amplitude (Fig. 4B), the time to peak value (TP) (Fig. 4C), and the rate of decrease (DT_{50}) (Fig. 4D) with respect to the control animals. Four weeks of sodium selenite treatment did alter neither the amplitude of the Ca^{2+} transients nor their kinetics of both TP and DT_{50}.

Comparative analysis of simulated and recorded action potentials

To be able to test our proposal related with sodium selenite treatment-induced slight prolongation in action potential duration is due to kinetic alterations in both Ca^{2+} and K^+ currents but not due to Ca^{2+} transients, we used our recorded data in the mathematical model of an action potential. We used -21.6 ± 1.6 (in the control group) and -15.7 ± 0.7 pA/pF (in the treated

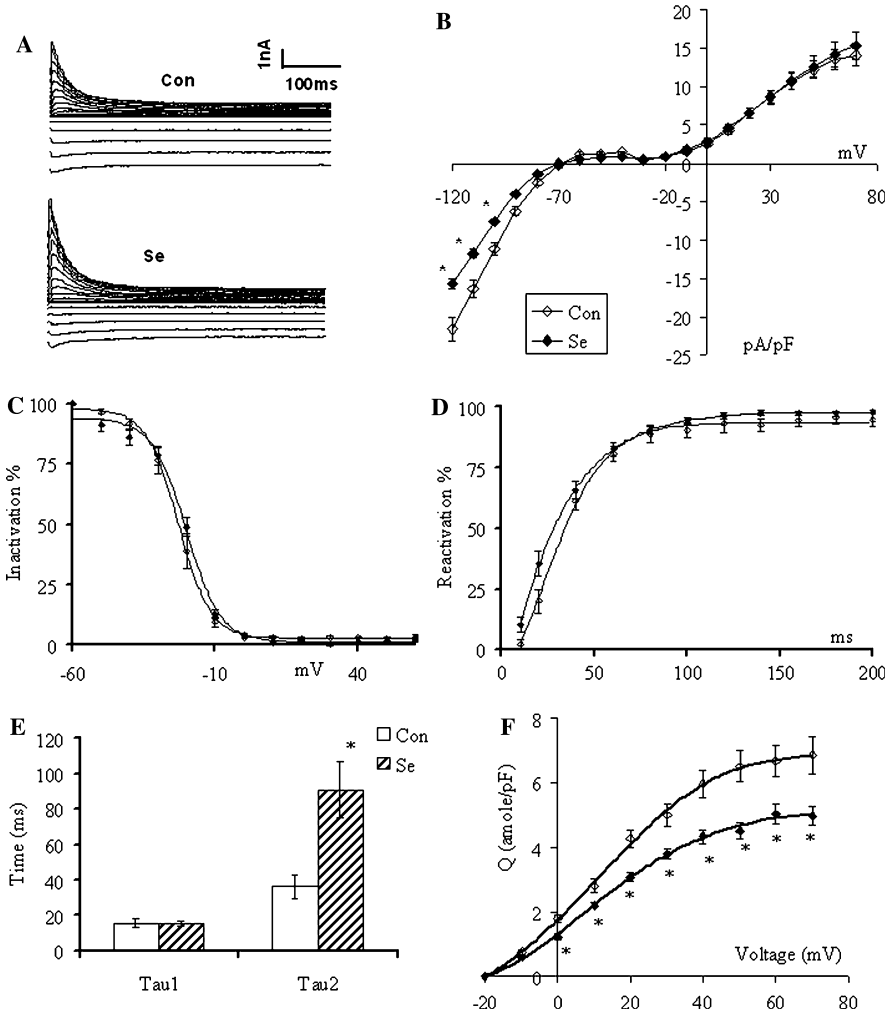

Fig. 3. Effect of sodium selenite treatment on the K^+ currents in ventricular cardiomyocytes. (A) Representative all K^+ currents recorded in cardiomyocytes from control (Con) and sodium selenite-treated rat (Se) hearts. Voltage pulses were applied from a holding potential of −80 mV to between −120 mV and +70 mV, with 10 mV steps (details in Materials and methods). (B) Current–voltage (*I–V*) relationships of peak I_K current in control (open triangles) and sodium selenite-treated control groups. (C) Graph is showing kinetics of the I_{to}. Steady-state inactivation curves obtained with two-pulse protocol. Holding potential was −80 mV. The currents resulting from the test pulse were normalized and plotted as a function of prepulse potential. (D) Time course of recovery from inactivation of I_{to} elicited with a two-pulse protocol is given. (E) The charge–voltage relationships between the groups. All values are represented as average ± SEM, $*p < 0.05$ with respect to the control group. *N*, number of animals and *n*, number of cardiomyocytes used current records are 5; 18 and 6; 20 in control and sodium selenite-treated groups, respectively.

group) for I_{K1} and 14.1 ± 1.4 pA/pF (in the control group) and 15.4 ± 1.8 pA/pF (in the treated group) for I_{to}. Inactivation time constants (fast and slow parts) for I_{to} were 24.5 ± 3.6 vs 20.4 ± 2.4 ms in control group vs the treated group and 135.3 ± 26.0 ms vs 81.0 ± 16.4 ms in control group vs the treated group in the simulated action potential. The densities of L-type Ca^{2+} currents, I_{CaL} used in this simulation (recorded in control group vs the treated group), were −11.0 ± 1.0 pA/pF vs −10.6 ± 1.7 pA/pF. Their both fast and slow time constants were 56.7 ± 7.4 vs 96.6 ± 15.9 ms and 7.2 ± 0.6 vs 13.3 ± 2.4 ms (in control group vs the treated group).

The comparison of these two action potentials (recorded and simulated) is given in Fig. 5. As can be seen from this figure, the simulated action potential curves of both control (A) and treated (B) groups were fitting very well to our recorded action potentials. From this comparison, it can be concluded that sodium selenite treatment has a slight but not statistically significant prolongation in action potential duration when it is used for 4 weeks. More importantly, this prolongation is due to significant alterations in the kinetics of both Ca^{2+} and K^+ currents which can cause important changes in the membrane permeability to these ions.

Effect of sodium selenite on redox state of the heart cells

Changes in antioxidant enzymes, SOD, GR, and GSHPx as well as lipid peroxide content of both the

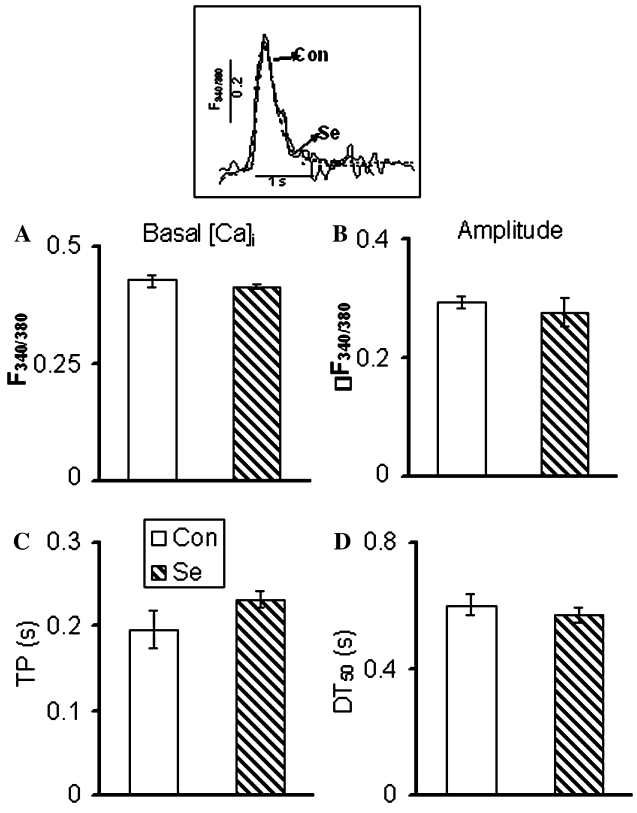

Fig. 4. Effect of sodium selenite on intracellular free Ca^{2+} changes. Representative Ca^{2+} transient traces obtained from cardiomyocytes of control (Con) and sodium selenite treated (Se) rats (5 μmol/kg/day for 4 weeks). Transients were induced by application of 20–30 V pulses with 10 ms duration at 0.2 Hz frequencies. Average basal ($F_{340/380}$) Ca^{2+} values, in (A) average amplitude of Ca^{2+} transients ($\Delta F_{340/380}$), in (B) average kinetic parameters of Ca^{2+} transients; time to peak in (C) and decay time to 50% of the peak in (D) are given. Data from control group were obtained from 5 rats and 15 cells while the treated group was 8 rats and 19 cells. All values are represented as average ± SEM.

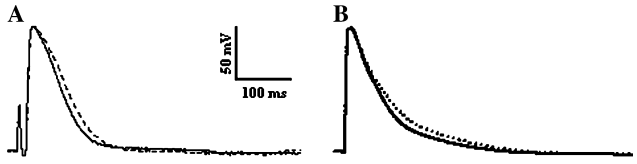

Fig. 5. Simulation of action potential. Action potential recordings from papillary muscles (A) and waveforms for model output (B) of the control (solid lines) and selenium-treated groups (dashed lines). Formulations for action potentials follow those of Pandit et al. [17,18] and Yaras and Turan [19].

control and sodium selenite treated rat hearts are shown in Table 2. There was a significant increase in GSHPx activity with no significant changes in the activities of the other enzymes in the list compared with the control group. Treatment of the rats with sodium selenite caused a significant increase in GSHPx activity, which has selenium as co-factor [1] even if there was no significant increase in plasma selenium level of the same group (Table 1). Sodium selenite treatment did cause neither lipid peroxidation nor an increase in the NO production in these hearts. As can be seen from Table 2, the NO products (NOPs) level in the treated group was not significantly different from the control group.

Although the total amount of glutathione did not change, the balance between GSSG and GSH changed significantly. GSH level decreased by about 13% and GSSG level increased by about 70% with sodium selenite treatment with respect to the untreated (control) group. This can indicate that sodium selenite treatment of the rats for 4 weeks caused an oxidation of the glutathione in the heart tissue and this oxidation order is very high with respect to the decline in the GSH level.

Discussion

In the present study, we have demonstrated that sodium selenite administration to the normal rats caused a slight but significant increase in blood glucose level, and a significant decrease in plasma insulin level. Here we showed also that there might be correlation between increased blood glucose and decreased plasma insulin levels and alterations in ionic mechanism of the cardiomyocytes together with alterations in the cell redox status and antioxidant defense system, even if there were no apparent deleterious changes in the heart functions.

In cell culture studies it has been demonstrated that sodium selenate increases glucose uptake in adipocytes and also increases the phosphorylation and activity of several signaling proteins activated by insulin [25–27]. On the other hand, Rasekh et al. [28] have shown that acute administration (ip) of sodium selenite to the rats caused hyperglycemia in a time- and dose-dependent manner. It has also been postulated that impaired insulin signaling and glucose utilization play major roles in electrical remodeling of the heart in diabetes mellitus and insulin treatment of the diabetic animals up-regulates I_{to} density to normal levels [29,30]. In this direction, Shimoni et al. [31] have reported that I_{to} channels are down-regulated in chronic disease states by alterations in transcription and surface expression of channel protein [32], and these cellular processes in the heart are under the control of the insulin signaling cascade [31]. Moreover, Xu et al. [29] have demonstrated the up-regulation of I_{to} channels by glutathione which is functionally coupled to insulin signaling in diabetic rat cardiomyocytes. Evidence from the present study suggests that oxidative stress and insulin signaling cascade couple was involved in the etiology of alteration of specific membrane currents. Reactive oxygen species, generated by intracellularly or exposed extracellularly, can induce membrane potential fluctuations [33], an early depolarization and prolongation in action potential duration [34], and alterations in K^+-, Ca^{2+}-, and Na^+-currents [33–39]. Although there are contradictories in

Table 2
Biochemical parameters of the heart tissue

	LPO (μM/g tissue)	NOPs (μM/g tissue)	GSH (μM/g tissue)	GSSG (μM/g tissue)	GR (mU/mg protein)	GSHPx (mU/mg protein)	SOD (mU/mg protein)
Control ($N = 8$)	0.49 ± 0.03	1.35 ± 0.19	6.82 ± 0.36	3.17 ± 1.03	2.58 ± 0.15	1.25 ± 0.14	0.67 ± 0.04
Se-treated ($N = 8$)	0.49 ± 0.07	1.29 ± 0.23	5.97 ± 0.29	5.40 ± 0.85*	2.94 ± 0.16	1.61 ± 0.20*	0.70 ± 0.18

Values are means ± SEM. Control group, saline-injected rats for four weeks; Se-treated group, sodium selenite-injected rats for four weeks. N represents the number of animals. LPO, lipid peroxidation; NOPs, nitric oxide products; GSH, reduced glutathione; GSSG, oxidized glutathione; GR, glutathione reductase; GSHPx, glutathione peroxidase; and SOD, superoxide dismutase.

* $p < 0.05$ is the significance levels compared to the control group.

the literature in terms of effect of the oxidant stress-induced alterations in these currents, most of the publications showed that both amplitude and activation/inactivation of I_{to} are modified by metabolic inhibition and oxidant stress. Besides its modulator function in the shape of cardiac action potential, I_{to} helps protect against arrhythmias. Some of the studies concluded that reactive oxygen species cause automaticity and hypercontracture in heart preparations due to an increased $[Ca^{2+}]_i$ via an increased I_{CaL} and Na/Ca exchange activity [33,34,37,39]. So, one can conclude that oxidant stress, in isolated cardiomyocytes, induces arrhythmogenic effects due to the modifications in amplitude and kinetics of membrane ionic currents. This hypothesis is supported with our present data. These observed effects of selenium compound on the kinetics and total carried charges by these two types of currents can be considered as a possible arrhythmogenic effect in heart preparations.

In the present study, we have shown that chronic administration of sodium selenite as micromolar concentration for 4 weeks caused some important alterations in the kinetics of both Ca^{2+}- and K^+-currents, even if there were no significant changes in the mechanical and electrical activities of the heart but apparent tendencies to prolong in the repolarizing phase of the action potentials. These alterations in the inactivation time constants of both currents could be correlated with these prolongations in the action potentials because the total charges carried by both currents were affected significantly with sodium selenite treatment. Using the measured kinetic values of both I_{to} and I_{CaL} in our modeling of the action potential, here in we have demonstrated that the slight prolongation in action potential repolarization phase can arise mostly due to the alterations in the kinetics of these currents.

Alterations of both I_{to} and I_{CaL} have been associated with altered action potential profiles and linked to changes in $[Ca^{2+}]_i$ and contractility [30,40–44]. Altered redox potentials can also profoundly affect cell function by modifying the structure and activity of proteins. Since the depletion of intracellular GSH, and the concomitant accumulation of GSSG is known to dramatically impair cell function through a shift in redox state of regulatory proteins and accumulation of GSSG in cells can promote the injurious oxidation of protein sulfhydryls [45], we may propose the same pathway to our results. Even though the underlying mechanisms of sodium selenite-mediated regulation of both Ca^{2+}- and K^+-channel activities are not fully understood by this hypothesis, the data given by Rozanski and Xu [46] seem to be in parallel with our present results. They showed that either external or internal application of GSSG leads to changes in I_{to} and demonstrated that GSSG levels are tightly controlled via specific transporters and the cell's redox state coupled to insulin-signaling cascade [47,48]. Another recent study also demonstrated that the insulin-signaling cascade can alter glutathione concentration in ventricular myocytes, and that these signaling mechanisms might play essential roles in controlling the intracellular redox state of cardiac myocytes [49]. So under these implications, our data show that sodium selenite can alter functions of these channels via a change in cell GSH levels due to increased blood glucose level and decreased plasma insulin level.

Alternatively, sodium selenite may increase the amount of NO release in the heart. However, our data indicated that sodium selenite treatment of the animals for four weeks did not change the NO products, were not changed in the heart tissue of the treated group, and so this possibility can be dropped.

In conclusion, our study shows some important alterations in the kinetics of the currents, which can lead to further more important alterations in the heart functions in further period, due to the effect of selenium on insulin-signaling cascade. Additional studies are needed on whether small doses of selenium compounds may be useful and/or as prooxidants when they are used as supplements in normal human diets.

Acknowledgments

We thank Dr. M. Ugur for his help in the evaluation of the data. This work was supported by grants from Ankara University Biotechnology Institute Research Fund and Ankara University Research Fund project 2003-08-09-98. Drs. B. Turan and G. Vassort were supported by a France-Turkish exchange program.

References

[1] J.T. Rotruck, A.L. Pope, H.E. Ganther, A.B. Swanson, D.G. Hafemen, W.G. Hoekstra, Selenium: biochemical role as a component of glutathione peroxidase, Science 179 (1973) 588–590.

[2] L.H. Foster, S. Sumar, Selenium in health and disease: A review, Crit. Rev. Food Sci. Nutr. 37 (1997) 211–228.

[3] L. Rao, B. Puschner, T.A. Prolla, Gene expressing profiling of low selenium status in the mouse intestine: transcriptional activation of genes linked to DNA damage, cell cycle control and oxidative stress, J. Nutr. 131 (2001) 3175–3181.

[4] J.T. Salonen, R. Salonen, K. Seppanen, S. Kantola, M. Parviainen, G. Alfthan, P. Maenpaa, Relationship of serum selenium and antioxidants to plasma lipoproteins, platelet aggregability and prevalent ischaemic heart disease in Eastern Finnish men, Atherosclerosis 70 (1988) 155–160.

[5] B. Turan, O. Hotomaroğlu, M. Kılıc c, E. Demirel-Yılmaz, Cardiac dysfunction induced by low and high diet antioxidant levels. Comparing selenium and Vitamin E in rats, Reg. Pharmacol. Toxicol. 29 (1999) 142–150.

[6] K. Sayar, M. Ugur, H. Gürdal, O. Onaran, O. Hotomaroglu, B. Turan, Dietary selenium and vitamin E intakes alter β-adrenergic response of L-type Ca-current and β-adrenoceptor-adenylate cyclase coupling, J. Nutr. 130 (2000) 733–740.

[7] R. Poltronieri, A. Cevese, A. Sbarbati, Protective effect of selenium in cardiac ischemia and reperfusion, Cardioscience 3 (1992) 155–160.

[8] S.Z. Imam, S.F. Ali, Selenium, an antioxidant, attenuates methamphetamine-induced dopaminergic toxicity and peroxynitrite generation, Brain Res. 855 (2000) 186–191.

[9] J.D. Overcast, A.E. Ensley, C.J. Buccafusco, C. Cundy, R.A. Broadnax, S. He, A.P. Yoganathan, S.H. Pollock, C.J. Hartley, S.W. May, Evaluation of cardiovascular parameters of a selenium-based antihypertensive using pulsed doppler ultrasound, J. Cardiovasc. Pharmacol. 38 (2001) 337–346.

[10] M. Ayaz, S. Ozdemir, M. Ugur, G. Vassort, B. Turan, Effects of selenium on altered mechanical and electrical cardiac activities of diabetic rat, Arch. Biochem. Biophys. 426 (2004) 83–90.

[11] S.Y. Lin-Shiau, S.H. Liu, W.M. Fu, Studies on the contracture of the mouse diaphragm induced by sodium selenite, Eur. J. Pharmacol. 167 (1989) 137–146.

[12] B. Turan, M. Desilets, L.N. Acan, O. Hotomaroglu, C. Vannier, G. Vassort, Oxidative effects of selenite on rat ventricular contractility and Ca movements, Cardiovasc. Res. 32 (1996) 351–361.

[13] M. Ugur, M. Ayaz, S. Ozdemir, B. Turan, Toxic concentration of selenite shortens repolarization phase of action potential in rat papillary muscle, Biol. Trace Elem. Res. 89 (2002) 227–229.

[14] B. Turan, M. Zhang, D. Prajapati, V. Elimban, N.S. Dhalla, Selenium protects against myocardial ischemia–reperfusion injury, J. Mol. Cell. Cardiol. 36 (2004) 764–765 (abstract).

[15] L.D. Koller, J.H. Exon, The two faces of selenium-deficiency and toxicity—are similar in animals and man, Can. J. Vet. Res. 50 (1986) 297–306.

[16] O. Casis, M. Gallego, M. Iriarte, J.A. Sanchez-Chapula, Effects of diabetic cardiomyopathy on regional electrophysiological characteristics of rat ventricle, Diabetologia 43 (2000) 101–109.

[17] S.V. Pandit, R.B. Clark, W.R. Giles, S.S. Demir, A mathematical model of action potential heterogeneity in adult rat left ventricular myocytes, Biophys. J. 81 (2001) 3029–3051.

[18] S.V. Pandit, W.R. Giles, S.S. Demir, A mathematical model of the electrophysiological alterations in rat ventricular myocytes in type-I diabetes, Biophys. J. 84 (2003) 832–841.

[19] N. Yaras, B. Turan, Interpretation of relevance of sodium–calcium exchange in action potential of diabetic rat heart by mathematical model, Mol. Cell. Biochem. (2004), in press.

[20] O.H. Lowry, N.J. Rosebrough, A.L. Farr, R.J. Randall, Protein measurement with the folin phenol reagent, J. Biol. Chem. 193 (1951) 265–275.

[21] C. Nebot, M. Moutet, P. Huet, J.Z. Xu, J.C. Yadan, J. Chaudiere, Spectrophotometric assay of superoxide dismutase activity based on the activated autoxidation of a tetracyclic catechol, Anal. Biochem. 214 (1993) 442–451.

[22] D.E. Paglia, W.N. Valentine, Studies on the quantitative and qualitative characterization of erythrocyte glutathione peroxidase, J. Lab. Clin. Med. 70 (1967) 158–169.

[23] J.A. Burns, J.C. Butler, J. Moran, M. George, G.M. Whitesides, Selective reduction of disulfides by Tris(2-carboxyethyl)phosphine, J. Org. Chem. 56 (1991) 2648–2650.

[24] G.L. Elmann, Tissue sulfhydryl group, Arch. Biochem. Biopysics. 82 (1959) 70–77.

[25] O. Ezaki, The insulin-like effects of selenate in rat adipocytes, J. Biol. Chem. 265 (1990) 1124–1130.

[26] S.R. Stapleton, G. Garlock, L. Foellmi-Adam, R.F. Kletzien, Selenium: potent stimulator of tyrosyl phosphorylation and activator of MAP kinase, Biochem. Biophys. Acta 1355 (1997) 259–269.

[27] Y.J. Hei, S. Farahbakhshian, X. Chen, M.L. Battell, J.H. McNeill, Stimulation of MAP kinase and S6 kinase by vanadium and selenium in rat adipocytes, Mol. Cell. Biochem. 178 (1998) 367–375.

[28] H.R. Rasekh, R.A. Potmis, V.K. Nonavinakere, J.L. Early, M.B. Iszard, Effect of selenium on plasma glucose of rats: role of insulin and glucocorticoids, Tox. Lett. 58 (1991) 199–207.

[29] Z. Xu, K.P. Patel, M.F. Lou, G.J. Rozanski, Up-regulation of K+ channels in diabetic rat ventricular myocytes by insulin and glutathione, Cardiovasc. Res. 53 (2002) 80–88.

[30] Y. Shimoni, H.S. Ewart, D. Severson, Type I and II models of diabetes produce different modifications of K^+currents in rat heart: role of insulin, J. Physiol. (London) 507 (1998) 485–496.

[31] Y. Shimoni, H.S. Ewart, D. Severson, Insulin stimulation of rat ventricular K^+ currents depends on the integrity of the cytoskeleton, J. Physiol. 514 (1999) 735–745.

[32] G.F. Tomaselli, E. Marban, Electrophysiological remodeling in hypertrophy and heart failure, Cardiovasc. Res. 42 (1999) 270–283.

[33] H. Matsuura, M.J. Shattock, Effects of oxidant stress on steady-state background currents in isolated ventricular myocytes, Am. J. Physiol. 261 (1991) H1358–H1365.

[34] R.I. Jabr, W.C. Cole, Alterations in electrical activity and membrane currents induced by intracellular oxygen-derived free radical stress in guinea pig ventricular myocytes, Circ. Res. 72 (1993) 1229–1244.

[35] H. Matsuura, M.J. Shattock, Membrane potential fluctuations and transient inward currents induced by reactive oxygen intermediates in isolated rabbit ventricular cells, Circ. Res. 68 (1991) 319–329.

[36] G.K. Pike, A.H. Bretag, M.L. Roberts, Modification of the transient outward current of rat atrial myocytes by metabolic inhibition and oxidant stress, J. Physiol. 470 (1993) 365–382.

[37] W.A. Coetzee, L.H. Opie, Effects of oxygen free radicals on isolated cardiac myocytes from guinea-pig ventricle: electrophysiological studies, J. Mol. Cell. Cardiol. 24 (1992) 651–663.

[38] A. Bhatnagar, S.K. Srivastava, G. Szabo, Oxidative stress alters specific membrane currents in isolated cardiac myocytes, Circ. Res. 67 (1990) 535–549.

[39] M. Tarr, D.P. Valenzeno, Modification of cardiac ionic currents by photosensitizer-generated reactive oxygen, J. Mol. Cell. Cardiol. 23 (1991) 639–649.
[40] D.W. Wang, T. Kiyosue, S. Shigematsu, M. Arita, Abnormalities of K^+ and Ca^{2+} currents in ventricular myocytes from rats with chronic diabetes, Am. J. Physiol. 269 (1995) H1288–96.
[41] J. Ren, J. Davidoff, Diabetes rapidly induces contractile dysfunctions in isolated ventricular myocytes, Am. J. Physiol. 272 (1997) H148–H158.
[42] D. Lagadic-Gossmann, K.J. Buckler, K. Le Prigent, D. Feuvray, Altered Ca2+ handling in ventricular myocytes isolated from diabetic rats, Am. J. Physiol. 270 (1996) H1529–37.
[43] K.M. Choi, Y. Zhong, B.D. Hoit, I.L. Grupp, H. Hahn, K.W. Dilly, S. Guatimosim, W.J. Lederer, M.A. Matlib, Defective intracellular Ca(2+) signaling contributes to cardiomyopathy in Type 1 diabetic rats, Am. J. Physiol. Heart Circ. Physiol. 283 (2002) H1398–408.
[44] T. Ishikawa, H. Kajiwara, S. Kurihara, Alterations in contractile properties and Ca2+ handling in streptozotocin-induced diabetic rat myocardium, Am. J. Physiol. 277 (1999) H2185–94.
[45] S.M. Deneke, Thiol-based antioxidants, Curr. Top. Cell Regul. 36 (2000) 151–180.
[46] G.J. Rozanski, Z. Xu, S.P. Didion, W.G. Mayhan, Metabolic basis of decreased transient outward K^+ current in ventricular myocytes from rats with experimental heart failure, Circulation 96 (2002) 1–7.
[47] D. Keppler, Export pumps for glutathione S-conjugates, Free Radic. Biol. Med. 27 (1999) 985–991.
[48] C.H. Foyer, F.L. Theodoulou, S. Delrot, The functions of inter- and intracellular glutathione transport systems in plants, Trends Plant Sci. 6 (2001) 486–492.
[49] S. Li, X. Li, G.J. Rozanski, Regulation of glutathione in cardiac myocytes, J. Mol. Cell. Cardiol. 35 (2003) 1145–1152.